1992A&A...259..333K

Astron. Astrophys. 259, 333–340 (1992)

ASTRONOMY AND ASTROPHYSICS

Interpretation of lightcurves of atmosphereless bodies

II. Practical aspects of inversion

M. Kaasalainen [1,2], L. Lamberg [3], and K. Lumme [1]

[1] University of Helsinki, Observatory and Astrophysics Laboratory, Tähtitorninmäki, SF-00130 Helsinki, Finland
[2] University of Oxford, Department of Theoretical Physics, 1 Keble Road, Oxford OX1 3NP, England
[3] University of Helsinki, Department of Mathematics, Hallituskatu 15, SF-00100 Helsinki, Finland

Received October 7, 1991; accepted January 9, 1992

Abstract. We have developed methods of inversion that can be used in the determination of the three-dimensional shape or the albedo distribution of the surface of a body from disk-integrated photometry, assuming the shape to be strictly convex (Kaasalainen et al. 1991, hereafter referred to as Paper I in the text and PI in the formulae). We also call this problem field photomorphography. In this second paper we study the practical aspects of the inversion procedure. We also apply our methods to lightcurve data of 39 Laetitia and 16 Psyche.

There are many observational factors having an influence on the outcome of inversion. Also, one must make some a priori assumptions that are used in the inversion process. The most important points are the number and range of the observing geometries, the assumed spin vector of the asteroid, possible large-scale nonconvexity of the surface, and the accuracy of the lightcurves.

In an appendix, we also describe how the formalism we have presented can be used in generating arbitary convex shapes conveniently and then in producing synthetic lightcurves efficiently with them.

Key words: asteroids – photometry – analytical methods

1. Introduction

In Paper I we presented the theoretical framework for photomorphography, largely leaving the practical aspects of lightcurve inversion to be discussed in this paper. The "real world" does not only provide observational data to be used in the inversion procedure; its properties are also introduced through some a priori assumptions and observational factors. Our purpose is to discuss points where the idealizations of the theory do not always hold true in practice. In some cases we offer a quantitative analysis, in others we present a more qualitative discussion. Also, our goal is to present general relationships and expressions rather than to engage in endless simulations. The main idea is to give a realistic picture of the practical points in applying photomorphographic methods to real data.

Send offprint requests to: M. Kaasalainen (University of Oxford)

First of all, the inverse problem is partly ill-posed, as we showed in Paper I. Therefore, the quantity and quality of observations being not ideal in practice, one must choose a proper technique for obtaining as reliable results as possible. In Paper I we recommended the Bayesian estimation theory in the form of the statistical inversion scheme. For completeness' sake, in Sect. 2 of this paper we give a brief description of how this method can be used in the inverse problem at hand.

In Sect. 3 we discuss the influence of the assumed spin vector of the asteroid. The values assumed for the rotation period and the pole position of the asteroid play, of course, a very important role in the inversion procedure. In Sect. 4 we discuss the effect of some other assumptions and observational factors: the range of the observing geometries, the accuracy of lightcurves, and the light-scattering law for the surface of the asteroid. Finally, in Sect. 5 we present inversion results for 39 Laetitia and 16 Psyche, and in this context discuss the role of the convexity assumption. In Sect. 6 we present our conclusions, and discuss the problems and possibilities in using photomorphographic techniques in practice. In Appendix B we give an algorithmical description of the usage of our formalism in producing synthetic lightcurves conveniently.

2. Use of Bayesian estimation theory in inversion

In this section we briefly present the use of statistical inversion theory in photomorphography problem. More detailed treatises on this method can be found in Menke (1984), Tarantola (1987), or Tarantola & Valette (1982).

Statistical inversion gives the result in the form of the so-called a posteriori probability density. Thus, in addition to the most probable solution, an error estimate is obtained. Also, by introducing an a priori distribution, this method can be used to regularize (see Paper I, Sect. 3) the solution to be stable if the problem is ill-posed. Consider a vector $\boldsymbol{y}$ representing measurements, and a vector $\boldsymbol{x}$ representing the free parameters of a theory predicting the measurements, i.e., $\boldsymbol{y} = \boldsymbol{f}(\boldsymbol{x}) + \boldsymbol{\varepsilon}$, $\boldsymbol{\varepsilon}$ being the measurement noise vector. If both $\boldsymbol{x}$ and $\boldsymbol{y}$ are considered as random variables with probability densities $D(\boldsymbol{x})$ and $D(\boldsymbol{y})$, and transition densities $D(\boldsymbol{y}|\boldsymbol{x})$ (meaning the probability of the measurements vector to be $\boldsymbol{y}$ when the parameter vector is $\boldsymbol{x}$) and $D(\boldsymbol{x}|\boldsymbol{y})$, the Bayes theorem states that

$$D(\boldsymbol{x}|\boldsymbol{y})\,D(\boldsymbol{y}) = D(\boldsymbol{x},\boldsymbol{y}) = D(\boldsymbol{y}|\boldsymbol{x})\,D(\boldsymbol{x}), \tag{2.1}$$

© European Southern Observatory • Provided by the NASA Astrophysics Data System

1992A&A...259..333K

where $D(\boldsymbol{x},\boldsymbol{y})$ is the joint probability density. From this it follows that the a posteriori probability density for $\boldsymbol{x}$ when the measurement vector is $\boldsymbol{y}$ is

$$D_{\mathrm{p}}(\boldsymbol{x}) = D(\boldsymbol{x}|\boldsymbol{y}) = CD_{\mathrm{pri}}(\boldsymbol{x})\, D(\boldsymbol{y}|\boldsymbol{x}), \tag{2.2}$$

where $D_{\mathrm{pri}}(\boldsymbol{x})$ is the a priori density for $\boldsymbol{x}$ (from some independent information), and the normalization coefficient $C = 1/\int D(\boldsymbol{x},\boldsymbol{y})\,\mathrm{d}\boldsymbol{x}$ (its value is irrelevant).

Let us now suppose that $\boldsymbol{\varepsilon}$ is a Gaussian zero-mean vector with covariance matrix Σ given by the expectation value $\langle \boldsymbol{\varepsilon}\boldsymbol{\varepsilon}^{\mathrm{T}} \rangle$. Then

$$D(\boldsymbol{y}|\boldsymbol{x}) = \frac{1}{(2\pi)^{N/2}|\Sigma|^{1/2}} \cdot \exp\left(-\frac{1}{2}(\boldsymbol{y}-f(\boldsymbol{x}))^{\mathrm{T}}\, \Sigma^{-1}(\boldsymbol{y}-f(\boldsymbol{x}))\right), \tag{2.3}$$

where N is the number of measurements and $|\Sigma|$ the determinant of Σ. Depending on the form of the function f and the a priori probability density, the a posteriori density for $\boldsymbol{x}$ may be written in a compact form.

A particularly convenient form is obtained with a linear theory. As we showed in Paper I (Sects. 3 to 5), the observed total brightnesses (or the Fourier coefficients of observed lightcurves) of a convex body are linearly related to a vector representing the shape and/or the surface light-scattering properties of the body, and we chose the components of this vector to be the coefficients of a truncated spherical harmonics series. In this case the relationship between $\boldsymbol{x}$ and $\boldsymbol{y}$ is

$$\boldsymbol{y} = A\,\boldsymbol{x} + \boldsymbol{\varepsilon}, \tag{2.4}$$

where A is a matrix operator representing the theory. Let us now take the a priori density for $\boldsymbol{x}$ to be also Gaussian with a centre point $\boldsymbol{x}_0$ and an error covariance matrix Σ_0:

$$D_{\mathrm{pri}}(\boldsymbol{x}) = C \exp\left(-\tfrac{1}{2}(\boldsymbol{x}-\boldsymbol{x}_0)^{\mathrm{T}}\, \Sigma_0^{-1}(\boldsymbol{x}-\boldsymbol{x}_0)\right), \tag{2.5}$$

C being a constant. In the case of a spherical harmonics series, $\boldsymbol{x}_0$ represents an a priori guess for the series and the diagonal elements of Σ_0 are the assumed variances of the coefficients, representing the possible deviations from the guess. Typically, a suitable a priori series is a sphere (thus only the first coefficient is nonzero) best describing the observations. The variances of the coefficients should be large enough to be able to represent irregular shapes; however, they should decrease as the degrees of the coefficients increase, in order to stabilize the solution (see Paper I, Sects. 4 and 5).

Equations (2.3), (2.4) and (2.5) can now be combined into the usual Gaussian form

$$D_{\mathrm{p}}(\boldsymbol{x}) = C \exp\left(-\tfrac{1}{2}(\boldsymbol{x}-\hat{\boldsymbol{x}})^{\mathrm{T}}\, Q\,(\boldsymbol{x}-\hat{\boldsymbol{x}})\right), \tag{2.6}$$

where the matrix Q (often called the Fisher information matrix) is

$$Q = \Sigma_0^{-1} + A^{\mathrm{T}}\Sigma^{-1}A, \tag{2.7}$$

and $\hat{\boldsymbol{x}}$, the centre point of the a posteriori distribution, is the most probable solution for the vector $\boldsymbol{x}$. It is given by

$$\hat{\boldsymbol{x}} = Q^{-1}(\Sigma_0^{-1}\boldsymbol{x}_0 + A^{\mathrm{T}}\Sigma^{-1}\boldsymbol{y}). \tag{2.8}$$

The variances (the squares of the errors) of the components x_k of $\boldsymbol{x}$ are the diagonal elements of the inverse of the matrix Q: $\sigma_k^2 = (Q^{-1})_{kk}$. Thus, in photomorphography, the inversion solution can be readily computed using Eqs. (2.7), (2.8) and a suitable a priori density. It might be of interest to note that if the a priori part is left out of the above equations, the result is the classical least squares solution to Eq. (2.4) (with Σ acting as a weighting matrix).

3. The spin vector

In Paper I we assumed the spin vector of the asteroid to be known so that the observation geometries can be computed. The shape/albedo part of the inversion is linear and can be represented in the form of Eq. (2.4), whereas the parameters describing the spin vector (rotation period and pole position) appear nonlinearly in the problem. Numerically, one can endeavour to solve this nonlinear part together with the linear part, as we describe later.

There are many proposed methods for obtaining the rotation period and pole position independently (see references in Paper I, Sect. 2). When such previously determined values for these parameters are used in photomorphographic analysis, it is, of course, very important to know how much errors in these values can affect the final result. We analyze this question in closer detail in this section.

First we study the effect of the assumed pole position of the asteroid. In the case of arbitrary observation geometries, a simple analytic expression for this cannot be found. However, we shall use a special geometry that, although restricted, represents most of the actual situations adequately. This will enable us to obtain a useful analytic solution that gives a picture of how an error in the pole position can affect the final result.

Consider an Earth-asteroid-Sun configuration such that the plane of the orbit of the asteroid lies in the plane of the ecliptic, and all the observations are made at opposition. The ecliptic latitude of the asteroid pole position is denoted by β; its ecliptic longitude is λ. The corresponding values for the assumed pole position are denoted by β' and λ'. In this example, $\beta' = 0$; thus the asteroid is assumed to be seen from all directions in the course of time. A unit vector of the pole position in a Cartesian coordinate system fixed to the ecliptic frame of reference is

$$\boldsymbol{P} = (\cos\beta\cos\lambda,\ \cos\beta\sin\lambda,\ \sin\beta)^{\mathrm{T}} \tag{3.1}$$

(and $\boldsymbol{P}'$ correspondingly for the primed variables). Now a unit vector toward the Earth from the asteroid can be written as

$$\boldsymbol{E} = (\cos\phi,\ \sin\phi, 0)^{\mathrm{T}}, \tag{3.2}$$

the angle ϕ representing the position of the Earth. Thus the cosine of the aspect angle θ between the line of sight and the rotation axis is

$$\cos\theta = \boldsymbol{E}\cdot\boldsymbol{P} = \cos\beta\cos(\lambda-\phi), \tag{3.3}$$

and again correspondingly for the primed variables. The angle ϕ can be eliminated from these two equations, resulting in

$$\begin{aligned}\cos\theta &= \cos\beta\cos\left[\lambda-\lambda' \pm \arccos\left(\frac{\cos\theta'}{\cos\beta'}\right)\right] \\ &= \frac{\cos\beta}{\cos\beta'}\left[\cos\theta'\cos(\lambda-\lambda') \pm (\cos^2\beta' - \cos^2\theta')^{1/2} \cdot \sin(\lambda-\lambda')\right].\end{aligned} \tag{3.4}$$

Let us now suppose that the ecliptic longitudes λ and λ' are equal or only a few degrees apart (usually the longitude of the pole position can be more accurately determined than the latitude). Then we have a simple relationship, at least to a high degree of accuracy, between the correct aspect angle and the incorrect one:

$$\cos\theta = c\cos\theta', \tag{3.5}$$

© European Southern Observatory • Provided by the NASA Astrophysics Data System

1992A&A...259..333K

where

$$c = \frac{\cos\beta}{\cos\beta'}. \tag{3.6}$$

Also, the absolute rotational phases φ and φ' (corresponding to the two pole positions) of the asteroid around its spin axis, as seen from the Earth, are equal (synodic corrections because of the orbital movement are certainly negligible). These relationships enable us to obtain the transformation describing the effect of the incorrect pole position on the result of the inversion.

As we showed in Paper I (Sect. 4), the total brightness of an asteroid at opposition can be written as a spherical harmonics (Laplace) series

$$L(\theta,\varphi) = \sum_{lm} K_l\, b_{lm}\, Y_l^m(\theta,\varphi), \tag{3.7}$$

where $K_l = 2\pi k_l$, k_l being defined in Eq. (PI: 4.8), and the coefficients b_{lm} describe the shape and/or albedo distribution of the surface. The same series can be written also for the incorrect pole position (primed variables and coefficients b'_{lm}); this represents the observations. Our goal is now to establish a transformation rule between the correct coefficients b_{lm} and the incorrectly deduced ones b'_{lm}.

Using (3.5), the series (3.7) becomes in the primed variables ($\varphi = \varphi'$)

$$L(\theta',\varphi') = \sum_{lm} K_l\, b_{lm}\, P_l^m(c\cos\theta')\, \mathrm{e}^{\mathrm{i}m\varphi'}, \tag{3.8}$$

where P_l^m is an associated Legendre polynomial. Using the orthogonality properties of spherical harmonics, this form can be transformed into the Laplace series form

$$L(\theta',\varphi') = \sum_{lm} K_l\, b'_{lm}\, Y_l^m(\theta',\varphi'). \tag{3.9}$$

This calculation is explicitly done in Appendix A. The main rule is that only such coefficients b'_{lm} and b_{lm} that have the same value for the index m and the same parity for the index l are interrelated. The result is

$$b'_{lm} = \sum_{p=m}^{L} C_{lp}^m\, b_{pm}, \tag{3.10}$$

where L is the largest degree included, and

$$C_{lp}^m = \frac{k_p}{k_l}\,\frac{2l+1}{2}\,\frac{(l+m)!}{(l-m)!}\, I_{lp}^m(c), \tag{3.11}$$

k_l defined in Eq. (PI: 4.8) and

$$I_{lp}^m(c) = \int_{-1}^{1} P_p^m(cx)\, P_l^m(x)\, \mathrm{d}x \tag{3.12}$$

calculated in Appendix A. (Note that if normalized spherical harmonics are used, the coefficient above has to be changed accordingly.)

From (3.10) it can be seen that, as a rule, if the error in the pole position is not larger than approximately 15°, the error in the inversion result will be practically negligible at least when the spherical harmonics series obtained is truncated early (as is the case in practice). If the pole position error exceeds 20° or so, the "mixing" between the coefficients b_{lm} becomes substantial, so the result obtained may not be very reliable.

Because lightcurves measured during a time interval of many years are used in inversion, the sidereal rotation period of the asteroid should be very accurately known if it is to be used in determining the absolute rotational phases. The extreme sensitivity of the inversion procedure to the rotational period is intuitionally quite clear. In order to compute the rotational phases to an accuracy of $\Delta\varphi$ over a time interval of t, the period T should be known to an accuracy

$$\Delta T = \frac{T^2\,\Delta\varphi}{t\,2\pi}. \tag{3.13}$$

If T is 10 h and t 10 yr, an accuracy of ten degrees would require ΔT to be 0.1 s. This can also be illustrated with the following example. Consider a situation where the difference $\Delta\varphi$ between the correct value φ and the assumed value φ' of the absolute rotational phase is a linear function of the aspect angle:

$$\Delta\varphi = \varphi - \varphi' = c\,\theta. \tag{3.14}$$

A physical configuration for this situation could be, for example, the same geometry as in the example for the pole position. Suppose that the pole of the asteroid lies in the plane of ecliptic and that at opposition the aspect angle is $\theta = (n/N)\,\pi$, where N and n are integers (N depends on the distance of the asteroid from the Sun and $n = 0, 1, \ldots, N$). Now the coefficient c in (3.14) is

$$c = \frac{2N+1}{T^2}\,\Delta T\, a, \tag{3.15}$$

where a denotes one year. From the $N+1$ oppositions, a spherical harmonics series describing the observations can be created. The value $N = 10$, for example, corresponds to an observation period of about 10 yr.

In the same manner as before, we can now derive a relationship between the coefficients b'_{lm} of the spherical harmonics series obtained using the erroneus value for the rotation period, and the actual coefficients b_{lm}. The result is of the same form as (3.10); in this case,

$$I_{lp}(c) = \int_0^{\pi} P_l^m(\cos\theta)\, P_p^m(\cos\theta)\, \mathrm{e}^{\mathrm{i}cm\theta}\, \sin\theta\, \mathrm{d}\theta. \tag{3.16}$$

This integral is straightforwardly calculated using, for example, (PI: B2); for $m = 0$, of course, $b'_{l0} = b_{l0}$. Using this result it is easy to see that if the rotation period is to be used in computing the rotational phases, it should be known at least to an accuracy of, typically, a couple of tenths of a second; otherwise the inversion result cannot be very reliable. In other words, the absolute rotational phases should be known to an accuracy of 20° or so.

If the rotation period is not known accurately enough, other methods must be used in determining the rotational phases correctly. An empirical result – having also some theoretical grounds – of the six best observed asteroids (Lumme et al. 1990), is that the phase difference between the first and the second order Fourier coefficients of a lightcurve exhibits no significant dependence on the aspect. Using this, the absolute phases can usually be determined within an accuracy limit of 20°. Another possibility is to use a series of small deviations from the a priori value and choose the result that gives the best fit in this series. If the surface of the asteroid is convex, this method may be able to provide the correct result quite distinctly: incorrect values for the period can quickly result in coefficients that make the spherical harmonics series obtained badly negative in some places. This technique can also be used for the pole position. Thus, using the best-fit and convexity criteria, the nonlinear parameters describing the spin vector can be deduced in addition to the linear parameters describing the surface.

© European Southern Observatory • Provided by the NASA Astrophysics Data System

1992A&A...259..333K

In this context we note that the assumption of relaxed, or nonprecessing, rotation can also be used as a further check on the result of the inversion. By computing the moment of inertia tensor (B2) one can check whether the rotation state of the shape solution is really relaxed or not, if this is not visually obvious. If the rotation axis is not aligned with the axis of the largest principal moment of inertia, and plausible density inhomogeneities removing this condition cannot be found, false assumptions have been used in the inversion. Mathematically it would be very difficult to incorporate this criterion in the inversion procedure as a constraint; thus it can usually be used only a posteriori as a check.

4. Other assumptions and observational factors

In addition to the rotational phase, there are three other angles defining an observing geometry in a coordinate system fixed to the asteroid. In what follows, we take these angles to be the aspect angle θ, the obliquity γ, and the solar phase angle α (see Paper 1, coordinate system $C2$ in Appendix A). The obliquity angle can be well covered, but the ranges of the aspect and solar phase angles are restricted by the pole position and the orbital geometry. Of these observational angles, the most important one is undoubtedly the aspect angle θ. Its values should reach well into both sides of the equator in order to display properly the features on the upper and lower parts of the object. The inversion procedure can naturally be carried out using any sets of data, as described in Sect. 2, but in order to obtain a stable and properly unambiguous solution, the range of the aspect angle should preferably be many tens of degrees. If the data are centred on the equatorial region, the solution will probably be badly north-south-ambiguous and thus not very meaningful.

The solar phase angle α also plays an important role when unambiguous solutions are wanted in the inversion. As we showed in Paper I, only nonzero phase angles can in practice provide information on the odd-degree coefficients (above degree one) of the Laplace series obtained in the inversion. The reason for this is the almost geometric light-scattering behaviour of dark solar system bodies at opposition. The fact is, however, that observations are best made near opposition and in any case the phase angles of asteroids are usually rather small, seldom over 30°. Can such phase angles provide valuable information so that it would be worthwhile to try to make observations as far away from opposition as possible?

In answering this question, we would first like to draw attention to the role of the obliquity angle γ. Its significance is, of course, coupled to the value of α. When α is very small, the effect of γ is in most cases certainly negligible. However, depending on the shape of the object, at larger phase angles (say, $\alpha > 15°$) γ may actually contribute rather significantly to the shape of the lightcurve. To see this, consider a cylindrical object, the shape of its end shown in Fig. 1. Let us assume that the observing geometries shown in the figure correspond to the two minima in the observed lightcurve. Also, let the scattering of light be geometric. At opposition or when the obliquity is $\gamma = 0°$ or $\gamma = 180°$, both minima are equal. However, because of the asymmetry of the object, the minima will be unequal if the illumination direction does not lie in the plane of the equator. The greatest difference is achieved when $\gamma = \pm 90°$. At $\alpha = 25°$, the intensity of the minimum corresponding to the elongated side will be only 5/8 of that at opposition, while the minimum intensity for the blunt side will be 9/10 of the opposition value. Thus there will be a 0.4 mag difference between the levels of the minima. The difference between the minima will vanish only when $\alpha = 0°$ or $\gamma = 0°/180°$. If the scattering is not geometric, the difference will prevail also at opposition.

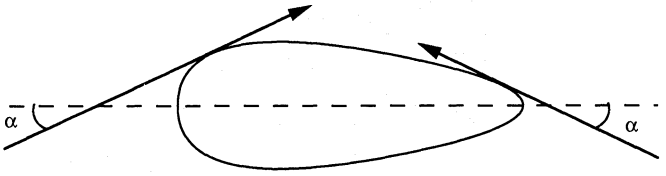

Fig. 1. Lightcurves at sufficiently large solar phase angles can differ significantly from those at zero angle, depending on the viewing geometry. In the figure, $\alpha = 25°$ and the dashed line represents the line of sight

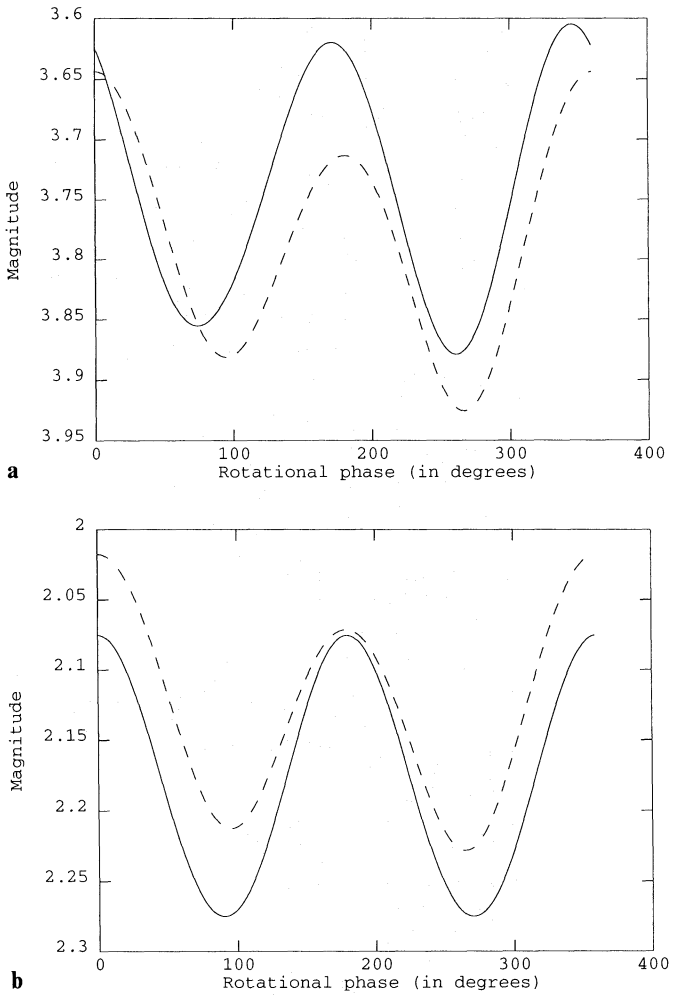

Fig. 2a and b. Lightcurves produced by the test object. **a** $\alpha = 0°$; solid line, $\theta = 90°$; dashed line, $\theta = 70°$. **b** $\alpha = 20°$, $\theta = 90°$; solid line, $\gamma = 0°$; dashed line, $\gamma = 90°$

The angles α and γ may thus have a significant effect on the shape of the lightcurve. If α is large enough, quite ordinary shapes can produce distinct effects. As an example of this, synthetic lightcurves produced by the test object in Paper I (shown in Fig. 1 therein) are shown in Fig. 2. The scattering law is the Lommel-Seeliger law, corresponding to geometric scattering at opposition. At opposition and $\theta = 90°$ the maxima equal each other as do the minima. Differences between maxima/minima can be produced at opposition if $\theta \neq 90°$, because the body is no longer viewed from

© European Southern Observatory • Provided by the NASA Astrophysics Data System

1992A&A...259..333K

opposite directions; in this case, $\theta = 70°$ (Fig. 2a). When $\theta = 90°$, $\alpha = 20°$ and $\gamma = 0°$, the lightcurve resembles mostly the one at $\alpha = 0°$. However, when the obliquity is changed to $\gamma = 90°$, distinct extrema differences appear (Fig. 2b). We want to stress the fact that no albedo variegation is needed to produce this lightcurve. Although at opposition and at equatorial aspect lightcurves of this kind would definitely imply albedo markings on the surface, at higher solar phase angles such implications are not self-evident.

Let us now investigate how the solar phase angle and the obliquity affect the actual coefficients obtained in inversion. At a fixed aspect angle, the integrated brightness of an asteroid can be written in the form of the Fourier series

$$L(\alpha, \gamma, \varphi) = \sum_m e^{im\varphi} \sum_l b_{lm} k_{lm}(\alpha, \gamma), \quad (4.1)$$

where φ is the rotational phase, and b_{lm}, as before, describe the surface features of the asteroid. The coefficients $k_{lm}(\alpha, \gamma)$ depend on the obliquity, the solar phase angle and the scattering law. The effect of the two angles can now be studied by computing $k_{lm}(\alpha, \gamma)$ for nonzero α values using the formulae derived in Sect. 5 of Paper I for general observation geometries.

Let us take the scattering law to be the Lommel-Seeliger law. In this case $k_{lm}(0, \gamma) = 0$ for all odd $l > 1$; thus the values of $k_{lm}(\alpha, \gamma)$ at odd l best express the potential value of nonzero solar phase angles. The general result is that, for example, $k_{3m}(\alpha, \gamma)$, vanishing at opposition, will be as large as $k_{4m}(\alpha, \gamma)$ only after the solar phase angle has exceeded about 15°, if the aspect angle θ is 30°. If $\theta = 45°$, this will happen around $\alpha = 20°$. At $\theta = 90°$ and $\gamma = 0°$ the effect of α on k_{3m} is negligible at obtainable phase angles; however, at $\gamma = \pm 90°$ it is as strong as at the aspect $\theta = 30°$ (cf. Fig. 2b). The coefficient k_{31} is influenced the most as α gets larger, as are the coefficients of the first order in general. Thus especially the coefficients b_{l1}, odd $l > 1$, are ones of which nonzero phase angles can provide information in inversion. Generally, the contribution of coefficients of odd $l > 1$ is best seen at nonequatorial aspect angles.

As an answer to the question of the practical importance of the solar phase angle, we can thus say that low-noise observations made at as large phase angles as possible can provide information unobtainable at opposition. In any case it must be noted that lightcurves obtained at phase angles over about 15° certainly no longer belong to the "near-opposition"-class. By this class we mean lightcurves that are principally determined by the aspect angle and in which the effect of α can adequately be explained by light-scattering phenomena. Such lightcurves (usually at $\alpha < 10°$) can often be extrapolated to $\alpha = 0°$ (Lumme et al. 1990) and then inverted in the same manner as Russell proposed (Paper I, Sect. 4). Although geometric scattering will leave some information unobtainable, its use in inversion may be better accounted for than assumptions for a scattering law at large phase angles.

The accuracy of the inversion result describing the surface features is, in the first hand, determined by the accuracy of the lightcurves. In other words, the magnitude of noise in the lightcurve data principally determines the truncation point of the spherical harmonics series obtained in inversion. As we noted in Paper I, the high-degree components of the shape or the albedo distribution contribute less to the total brightness than low-degree components. This is easily seen, for example, from Eqs. (PI: 4.12)–(PI: 4.14). Thus, information of the high-degree components of the shape is easily drowned in the noise. In practice, a typical truncation point is at degree 4, which is enough to provide a coarse description of the global shape.

An important a priori assumption used in the inversion process is the light-scattering law for the surface of the asteroid. In Paper I, we showed that theoretically it is possible to deduce free parameters in the scattering law at the same time as the parameters describing the shape (or the albedo distribution) are determined. However, as we pointed out, the number of observations needed is very large and thus, in practice, a detailed assumption for the scattering law must be used. The best method is probably to seek the best fit using a few different values for the scattering parameters, much in the same way as the best fit for the spin vector could be searched for.

5. Applications to real data; convexity assumption

A thorough photomorphographic analysis of an object is a somewhat laborious task. The computation itself is, of course, quite straightforward, as we showed in Paper I and Sect. 2 of this paper. The practical problems are associated with the points we have described above. For example, first one has to compile all the lightcurve measurements of the object and perhaps discard some of them; then the pole position and the absolute rotational phases of the lightcurves should be determined. If the lightcurves do not properly lend themselves to Fourier analysis e.g. because of gaps in data, individual lightcurve points must be used in the equation of statistical inversion (Sect. 2). Also, one has to decide what scattering law is to be used and at which point to truncate the Laplace series obtained in the inversion. After obtaining the coefficients of this series, the result must be interpreted. Are considerable albedo variations a possibility? If the sum of the series produced substantially negative values, should some of the a priori assumptions be changed, or is the surface considerably nonconvex? If different values for the spin vector and/or scattering law are used, all this will have to be repeated many times over. To automatize the whole procedure would be very difficult, so a substantial amount of individual labour is indeed required.

It is not in the scope of this paper to undertake the complete aforementioned task. Instead, to illustrate some of the practical aspects typical for this inversion problem, we used some data previously processed and analyzed for convenient use. Such data are the Fourier coefficients for some lightcurves of 39 Laetitia and 16 Psyche obtained at various observing geometries (Lumme et al. 1992), and the pole positions for these asteroids, computed using the spherical harmonics method (Lumme et al. 1990, 1992). Because Fourier series were used, the inversion was cast in the form of Eq. (PI: 5.11).

For 39 Laetitia, 16 lightcurves were used (aspect angle ranging from 41° to 151° and solar phase angle from 6° to 23°); for 16 Psyche, 18 lightcurves ($17° \leqq \theta \leqq 150°$ and $2° \leqq \alpha \leqq 21°$), ten of which were concentrated within an aspect interval of a few degrees. The scattering law used was a combination of the Lommel-Seeliger law and Lambert's law (relative contributions of 1 and 0.3, respectively) with solar phase functions as in the Lumme-Bowell law (Lumme et al. 1990). It was found that the final result was rather insensitive to the relative contributions of the two scattering laws; the chosen combination gave the best fit.

Both spherical harmonics series describing the outcomes of inversion were truncated at degree four because of the magnitude of noise in data. For 39 Laetitia, the degree one coefficients were very close to zero; thus no substantial albedo features were indicated, and the result could well be taken to describe shape. In the case of 16 Psyche, albedo variegations are more probable but still minor compared to the shape effects.

© European Southern Observatory • Provided by the NASA Astrophysics Data System

1992A&A...259..333K

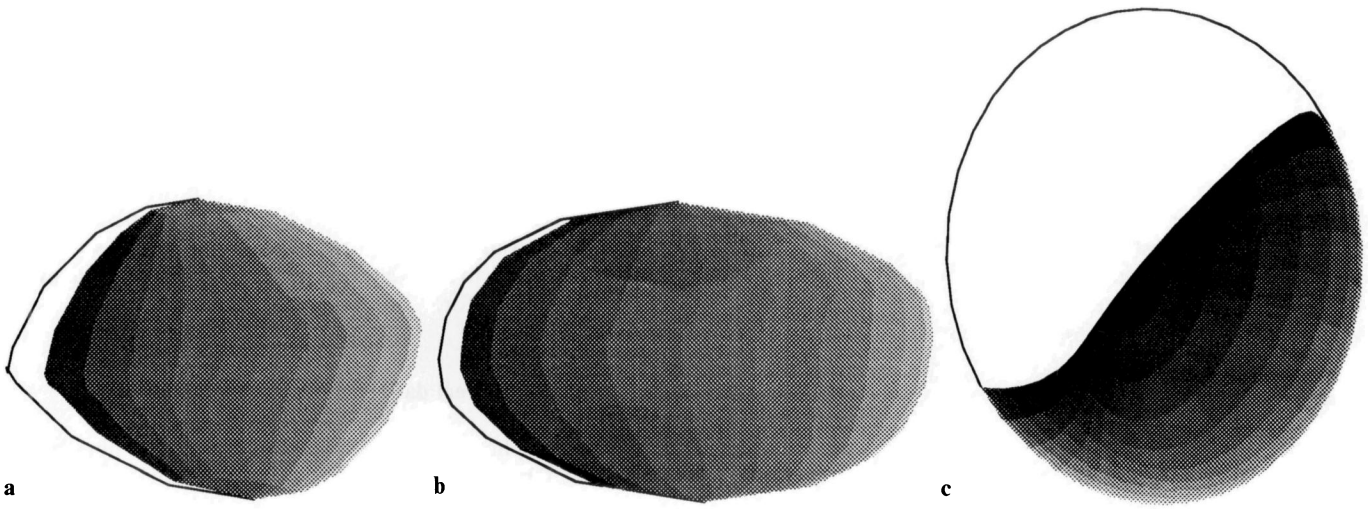

Fig. 3a–c. The shape solution for 39 Laetitia, shown as viewed from three mutually perpendicular directions. The shadowed part of the limb is also shown. The direction of the rotation axis is vertical in **a** and **b**; in **c** the body is viewed from directly above such that the viewing directions corresponding to **a** and **b** are, respectively, directly below and on the right-hand side of **c**. In **a** and **b** the solar phase angle is 30°, the illumination direction being perpendicular to the rotation axis; in **c** the illumination direction is the same as in **a**

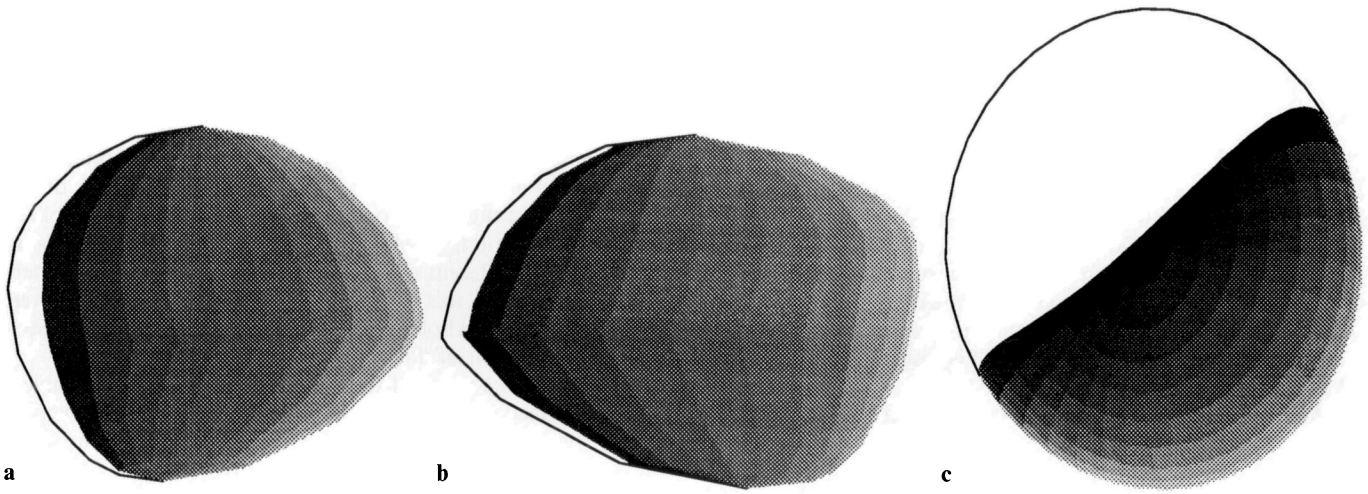

Fig. 4a–c. The shape solution for 16 Psyche, shown in the same manner as 39 Laetitia in Fig. 3

In Fig. 3 the shape result for 39 Laetitia is shown as viewed from three mutually perpendicular directions. In Figs. 3a and b the viewing directions are perpendicular to the rotation axis which is pointing upwards in the plane of the paper; in Fig. 3c the body is viewed from directly above so that the viewing directions corresponding to Figs. 3a and b are, respectively, directly below and on the right-hand side of Fig. 3c.

In Figs. 3a and b the solar phase angle is 30°, the illumination direction being perpendicular to the rotation axis; in Fig. 3c the illumination direction is the same as in Fig. 3a. The images were produced in the same manner as the ones in Paper I; for more detailed description, see notes therein. Figure 4 represents the shape result of 16 Psyche in the same manner as with 39 Laetitia.

The obtained solutions fitted the original data to an average accuracy of about two percent, corresponding to about 0.02 mag. It should be noted that the results are the *convex* shapes best reproducing the original data with the assumptions for the scattering law and spin vectors. Better fits would have produced substantially negative values for the sums of the series obtained in inversion, thus resulting in solutions unable to provide quantitative shape descriptions. In both cases nonconvexities are possible, but convex surfaces can probably describe the global shapes adequately.

Generally, it would seem that if the observed body is globally nonconvex, the inversion procedure will produce inconsistent results and thus reveal the character of the object. In fact, objects that are not strictly convex but still convex, i.e. objects having planar sections, can already induce such results because of the truncation of the spherical harmonics series obtained in inversion. Lightcurves of convex polyhedra are easy to compute in order to simulate such cases. If, for example, a brick-shaped body is used to produce lightcurves in the same observing geometries as for 39 Laetitia above, a convex solution reproducing the lightcurves acceptably cannot be found unless the truncation degree is unpractically high. Even if negative values are allowed for the spherical harmonics series obtained in inversion and the highest

© European Southern Observatory • Provided by the NASA Astrophysics Data System

1992A&A...259..333K

degree is 8, the lightcurves reproduced by this series will not be able to produce a good fit. The truncation point thus, in a way, sets a limit for the class of shapes that can be recovered in inversion.

In order to properly investigate the effect of globally nonconvex bodies, lightcurves produced by such objects should numerically be computed for simulations. This, however, is a rather time-consuming task requiring a proper ray-tracing code. At this stage, we are content with the aforementioned results. At opposition, lightcurves of a nonconvex body can be quickly computed if the scattering law is assumed to be geometric: the total brightness is simply the area inside the apparent boundary curve of the object, which is easy to compute numerically. We have done some simulations using this method, and the results seem to support the conclusion that the inversion methods using convexity assumption may not be able to give a reasonable solution (for example the convex hull of the surface) if the object is globally nonconvex.

6. Conclusions and discussion

We have discussed in closer detail the practical aspects of lightcurve inversion that we only briefly mentioned in Paper I. To sum up, the most important points are:

(1) The assumed spin vector of the asteroid. The inversion procedures are not too sensitive to the pole position, as long as it is known to an accuracy of about 15°. The absolute rotational phases should be known to the same accuracy as the pole position.

(2) The number and the range of the observing geometries. Especially the aspect angle should extend well outside the equatorial zone; if this is not possible, the solution obtained tends to be numerically not well determined. Nonzero solar phase angles can in principle provide information unobtainable at opposition if the scattering of light is geometric there. In practice, obtaining this information is difficult because of the small phase angles. Accurate observations as far away from opposition as possible are required; also, the light-scattering law should be well known. Aspect angles far from equator, or equatorial aspects when the illumination direction is not near the equatorial plane, are best for this purpose.

(3) The accuracy of lightcurves. The magnitude of noise in the lightcurve data primarily determines the truncation point of the spherical harmonics series obtained in inversion. This stems from the fact that high-degree components of the shape contribute less to the total brightness than low-degree ones. A typical truncation point is at degree 4, which is enough to provide a coarse description of the shape.

(4) The convexity of the surface. If the surface is globally nonconvex, the inversion procedure cannot obtain a description of its shape. However, an indication of nonconvexity can be obtained. Local nonconvex features, such as craters, often make no significant contributions to lightcurves and are thus no real obstacles for inversion under the convexity assumption. For globally nonconvex objects there probably is no analytical or "numerically algorithmic" inversion scheme.

This paper concludes our presentation of the theory of lightcurve inversion under convexity assumption. Lightcurves can provide enough information for obtaining the global shape of the object even though some assumptions used in the theory would not completely hold true in practice. A proper inversion analysis requires systematic and planned observations of the chosen target in order to collect a sufficient number of lightcurves at suitable observing geometries. Naturally, the most economical way would be to continue observing some of the best-observed asteroids so far, but these matters we leave to be discussed among those whom the practical implementation may concern.

Acknowledgements. We would like to thank Karri Muinonen for useful discussions and Hannu Karttunen for providing the Fourier coefficients of the lightcurves of 39 Laetitia and 16 Psyche.

Appendix A

The function (3.8) can be transformed into the Laplace series (3.9) by using the orthogonality properties of spherical harmonics (Paper I, Appendix B). Thus an integral of the form

$$\int_0^{2\pi}\int_0^{\pi} \sum_{pn} B_{pn} P_p^n(c\cos\theta)\, e^{in\varphi} P_l^m(\cos\theta)\, e^{-im\varphi} \sin\theta \, d\theta \, d\varphi \qquad (A1)$$

(B_{pn} a complex-valued coefficient) has to be calculated in order to obtain the coefficients b'_{lm} of (3.9). First, the φ integral gives a nonzero value 2π only when $n = m$, thus fixing this index. Next, we calculate the integral

$$I_{lp}^m(c) = \int_{-1}^{1} P_p^m(cx)\, P_l^m(x)\, dx. \qquad (A2)$$

From the parity properties of P_l^m it follows that this integral vanishes when p and l are not of the same parity, i.e., are not both even or both odd. Using (PI: B2)–(PI: B4) we can write

$$\begin{aligned} I_{lp}^m(c) &= \sum_{n=0}^{l-m}\sum_{k=0}^{p-m} c^k A_{lm}^n A_{pm}^k \\ &\quad \cdot \int_{-1}^{1} x^{k+n}(1-x^2)^{m/2}(1-c^2x^2)^{m/2}\, dx \\ &= \sum_n \sum_k \sum_{i=0}^{M/2}\sum_{j=0}^{M/2} \\ &\quad \cdot c^{k+2j} A_{lm}^n A_{pm}^k \binom{M}{i}\binom{M}{j}(-1)^{i+j} J(s), \end{aligned} \qquad (A3)$$

where $s = (k+n)/2 + i + j$ ($k+n$ is always even for nonvanishing combinations of the A-coefficients). For even and odd m, respectively, $M = m/2$, $J(s) = 2/(2s+1)$, and $M = (m-1)/2$,

$$J(s) = \int_{-1}^{1} x^{2s}[(1-x^2)(1-c^2x^2)]^{1/2}\, dx, \qquad (A4)$$

which for numerical evaluation can be written, substituting $x = \cos\theta$ and using the Taylor expansion, as

$$\begin{aligned} J(s) = \pi\Bigg[&\frac{(2s-1)!!}{(2s)!!\,(2s+1)} - \sum_{n=1}^{\infty} \frac{c^{2n}}{(2n-1)} \\ &\cdot \frac{(2n-1)!!}{(2n)!!} \frac{[2(n+s)-1]!!}{[2(n+s)]!!} \frac{1}{2(n+s+1)}\Bigg]. \end{aligned} \qquad (A5)$$

The series converges when $c < 1$. Substituting these results back into (PI: B9), the relationship (3.10) between the coefficients b'_{lm} and b_{lm} is obtained.

Appendix B: synthetic lightcurves

We describe here algorithmically how our formalism can be used in producing synthetic lightcurves of convex bodies. All the

© European Southern Observatory • Provided by the NASA Astrophysics Data System

1992A&A...259..333K

necessary formulae are given here and in Paper I, and it is a very straightforward task to represent the mathematics in any programming language. An external subroutine is needed for numerical integration; since this is a very well studied problem, there are numerous standard procedures readily available in different subroutine packages (e.g. NAG) or in the literature (e.g. Press et al. 1986). This method is very optimal, since the lightcurves can immediately be given in the form of Fourier coefficients (rather than computing one brightness value at a time), and the computation time is very short. Another advantage is the possibility to conveniently create and use arbitrary convex shapes instead of ones merely based on "standard", e.g. ellipsoidal, figures.

The outline of the algorithm is quite simple: all strictly convex bodies can be described using the support function or the Gaussian surface density (see Paper I, Appendix C). A convex shape is most conveniently created by giving a suitable support function. From this the Gaussian surface density is easily computed and then readily used in determining integrated brightnesses in any observing geometries with a chosen scattering law.

Creating convex bodies

All functions on the surface of a body are here given in the form of a spherical harmonics series; thus the first task is to find such a series describing the support function of a chosen shape. Interestingly enough, there is no immediately obvious way for doing this in practice, and there are many possibilities. After having tried various manners of approach, we have found the following method by far the easiest.

In order to be able to produce sufficiently irregular bodies, we use the fact that support functions are additive: if two support functions describing strictly convex bodies are added together, the result is also a support function. We start with a droplet-shaped surface of revolution that is formed by rotating around the z-axis a half-parabola $y = C - az^2$ above the xy-plane and a quarter-circle $y^2 + z^2 = C^2$ below the xy-plane; the width and height of the droplet are thus $2C$ and $C + (C/a)^{1/2}$, respectively. This surface can be parametrized using the polar angle ϑ of its surface normal. In the beginning of the parabola at the top of the droplet, $\vartheta = \vartheta_0 = \arctan \frac{1}{2}(Ca)^{-1/2}$. The support function (PI: 6.1), independent of the azimuthal angle ψ, is now

$$\varrho(\vartheta) = \begin{cases} (C/a)^{1/2} \cos\vartheta, & 0 \leqq \vartheta < \vartheta_0 \\ C \sin\vartheta + \dfrac{\cos^2\vartheta}{4a \sin\vartheta}, & \vartheta_0 \leqq \vartheta < \frac{\pi}{2}. \\ C, & \frac{\pi}{2} \leqq \vartheta \leqq \pi \end{cases} \quad \text{(B1)}$$

This function can be transformed into a spherical harmonics series (PI: B8) by integrating numerically Eq. (PI: B9). The series contains only $m = 0$ terms, and the truncation degree is determined by the "sharpness" of the droplet and the accuracy wanted; typically there is no need to exceed, say, degree 8 or 10. The resulting series need not describe the droplet exactly: the idea is just to produce a suitable shape that can be used in constructing irregular surfaces. The coefficients of degree 1 can be ignored, since they represent only a translation.

Arbitrary convex bodies can now be created by rotating the obtained series using Eq. (PI: B10) and various Euler angles, thus producing "tilted" droplets, and by adding the rotated functions together: various droplet shapes and weight factors can, of course, be used. The shape corresponding to the resulting support function can be drawn using (PI: C3)–(PI: C5). Using a suitable computer graphics package one can experiment with different droplet combinations very conveniently. Note carefully that the z-axis always represents the rotation axis of the body; if needed, the moment of inertia tensor I can be computed in terms of the support function from

$$I_{ij} = \frac{1}{5} \int_0^{2\pi} \int_0^{\pi} \left(\delta_{ij} \sum_{k=1}^{3} r_k^2 - r_i r_j \right) \varrho(\vartheta, \psi)\, G(\vartheta, \psi) \sin\vartheta \, \mathrm{d}\vartheta \, \mathrm{d}\psi \quad \text{(B2)}$$

(assuming a homogeneous density distribution), where G is computed from (PI: C10) and (PI: C11) and the Cartesian components r_i of the radius vector of the surface are obtained from (PI: C5). This matrix can then be diagonalized, and the support function can be rotated accordingly so that the rotation axis will be consistent with the assumption of relaxed rotation.

Integrated brightness

Once a support function describing a suitable body is found, its Gaussian surface density is readily computed using (PI: C10) and (PI: C11). This function is then again transformed into a spherical harmonics series integrating (PI: B9). This can be done completely analytically using (PI: B2)–(PI: B4); the integrand comprises then straightforwardly integrable combinations of sines and cosines. It is recommendable to compute the integrals of these combinations in a file ready to be used; this reduces the computation time especially with long spherical harmonics series. The truncation degree of the series describing the Gaussian surface density usually need not be larger than that of the support function series. Of course, the effect of the truncation point on the accuracy of the series representation should always be checked.

Since lightcurves produced by a triaxial ellipsoid can be useful also in this scheme, we note that using the formulae in Appendix C of Paper I one can calculate the Gaussian surface density of a triaxial ellipsoid with semimajor axes a, b, c to be

$$G(\vartheta, \psi) = \left(\frac{a}{bc} \sin^2\vartheta \cos^2\vartheta + \frac{b}{ac} \sin^2\vartheta \sin^2\psi + \frac{c}{ab} \cos^2\vartheta \right)^{-2}, \quad \text{(B3)}$$

the rotation axis being aligned with the c-axis.

When the Gaussian surface density is known and the scattering law has been chosen, the integrated brightnesses follow immediately from (PI: 4.7) (opposition geometry) or (PI: 5.6) (general geometry). These formulae provide the Fourier coefficients of a complete lightcurve obtained in any chosen observing geometry; the angles defining the geometry are easily computed using Appendix A of Paper I. Depending on the form of the scattering law, some numerical integration is often needed especially in (PI: 5.6).

References

Kaasalainen M., Lamberg L., Lumme K., Bowell E., 1991. A&A 259, 318

Lumme K., Karttunen H., Bowell E., 1990, A&A 229, 228

Lumme K., Karttunen H., Bowell E., 1992 (in preparation)

Menke W., 1984, Geophysical Data Analysis, Academic Press, New York

Press W., Flannery B., Teukolsky S., Vetterling W., 1986, Numerical Recipes. Cambridge University Press, Cambridge

Tarantola A., 1987, Inverse Problem Theory – Methods for Data Fitting and Model Parameter Estimation. Elsevier, Amsterdam

Tarantola A., Valette B., 1982, J. Geophys. 50, 159

© European Southern Observatory • Provided by the NASA Astrophysics Data System